Systematic analysis of direct-drive baseline designs for shock ignition with the laser MegaJoule

Brandon V.[1], Canaud B.[1,a], Laffite S.[1], Temporal M.[2], and Ramís R.[2]

[1] CEA, DAM, DIF, F-91297 Arpajon, France
[2] ETSIA, Universidad Politécnica de Madrid, Spain

Abstract. Direct-drive inertial confinement thermonuclear fusion consists in illuminating a shell of cryogenic Deuterium and Tritium (DT) mixture with many intense beams of laser light. Capsule is composed of DT gas surrounded by cryogenic DT as combustible fuel. Basic rules are used to define shell geometry from aspect ratio, fuel mass and layers densities. We define baseline designs using two aspect ratio (A=3 and A=5) who complete HiPER baseline design (A=7.7). Aspect ratio is defined as the ratio of ice DT shell inner radius over DT shell thickness. Low aspect ratio improves hydrodynamics stabilities of imploding shell. Laser impulsion shape and ablator thickness are initially defined by using Lindl (1995) pressure ablation and mass ablation formulae for direct-drive using CH layer as ablator. In flight adiabat parameter is close to one during implosion. Velocities implosions chosen are between 260 km/s and 365 km/s. More than thousand calculations are realized for each aspect ratio in order to optimize the laser pulse shape. Calculations are performed using the one-dimensional version of the Lagrangian radiation hydrodynamics FCI2. We choose implosion velocities for each initial aspect ratio, and we compute scaled-target family curves for each one to find self-ignition threshold. Then, we pick points on each curves that potentially product high thermonuclear gain and compute shock ignition in the context of Laser MégaJoule. This systematic analyze reveals many working points which complete previous studies allowing to highlight baseline designs, according to laser intensity and energy, combustible mass and initial aspect ratio to be relevant for Laser MégaJoule.

1 Introduction

Inertial confinement fusion (ICF) is a main approach to exploit thermonuclear energy in civilian energy production [1–4]. ICF principle consists in illuminating a shell of fusible fuel directly with laser beams in direct-drive approach [1,5,6] or with x-ray in indirect drive approach [2, 4]. Two laser facilities are built to realized ICF with indirect drive configuration : the National Ignition Facility (NIF) in U.S. [7] and the Laser MégaJoule (LMJ) in France [8]. Canaud *et al.* [9] demonstrated that it is possible to self-ignite a capsule with indirect-drive beam geometry design of LMJ. Moreover, shock ignition scheme [10] and it application on LMJ [11] bring a new interest for direct-drive approach because it can offer high gain and a best laser capsule coupling. In this scheme, compression phase and ignition are separated.

Actually, targets designs present high aspect ratio around A=7 as HiPER target [12] if we consider only payload fuel of this target, this aspect ratio value is harmful for hydrodynamic stability and target hardiness during implosion phase that reach high implosion velocities. In our study, we explored two targets designs baselines to increase hydrodynamic stability and lower implosion velocities. We fixed aspect ratio at 3 and 5 and searched target design for large range of implosion velocities that will present in first part. We chose working point in function of implosion velocities, areal densities and thermonuclear energies and computed scaled target in second part, and we shock-ignited specific points to reach high gain.

[a] e-mail: benoit.canaud@cea.fr

2 Direct-drive baseline designs

We explored shells designs composed by DT (Deuterium-Tritium) gas surrounded by 300 μg cryogenic DT fuel with a CH ablator layer for Laser MégaJoule (LMJ). CH is more efficiently as ablator than DT. We defined two targets geometries with lower aspect ratio than HiPER target. Aspect ratio choosen, defined as ratio between interior fuel radius and fuel thickness, have value of 3 and 5. Targets designs with lower initial aspect ratio is interesting to reduce hydrodynamics instabilities and exploring lower implosion velocities at laser energy fixed. Targets geometries are presented in Figure 1. CH ablator thickness was defined using Lindl formulae [2] with ablation pressure (P_{abl} = 300 GPa) and implosion velocities expected (310 km/s) considerations :

$$p_a(\mathrm{Pa}) = 40\,.10^{-3}\left(\frac{(\mathrm{W/m^2})\,.10^{-4}}{\lambda(\mathrm{m})}\right)^{\frac{2}{3}} \qquad (1)$$

$$\dot{m}_a(\mathrm{kg/m^2/s}) = 2.6\,.\,10^{-7}\left(\frac{(\mathrm{W/m^2})\,10^{-4}}{\lambda^4(\mathrm{m})}\right)^{\frac{1}{3}} \qquad (2)$$

Calculations are performed using the one-dimensional (1D) Lagrangian radiation-hydrodynamics code : FCI 1D [13] usually used for ICF design studies at CEA, DIF. It includes tabulated equations of state (e.g. SESAME), flux-limited Spitzer heat transport (here the flux limiter is set at 6%), multi-group radiative transfer, 1D normal-incidence ray-tracing with refraction, multi-group alpha-particle transport and neutron transport. Degeneracy of the fuel during the deceleration is taken into account in the thermal conductivity using a harmonic average between Spitzer and the Hubbard (1966) [14] model that is validated by quantum molecular dynamics calculations [15]. However, we used SESAME equation of state for DT, but the new equation of state recently calculated by Caillabe *et al.* [16] will be used in the future.

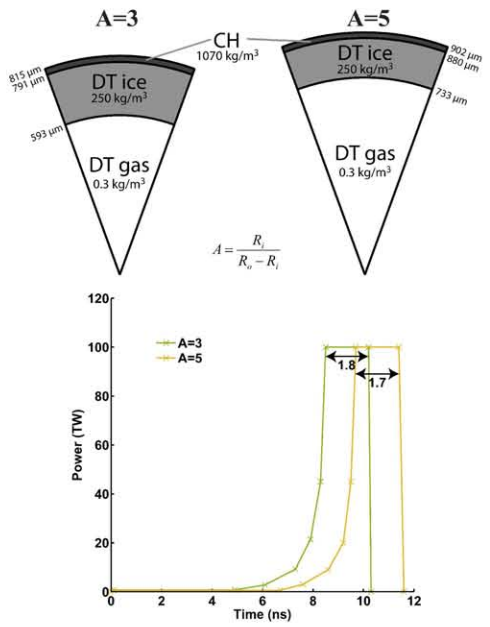

Fig. 1. Targets geometries designed with low aspect ratio A=3 and A=5 (top). Laser pulses shapes initially defined to be associated to targets geometries for aspect ratio A=3 (green) and A=5 (yellow).

Laser pulses shapes are defined to reach implosion velocities around 310 km/s for each design and follow a Kidder like law [17] to minimize entropy during compression phase. We tried to keep adiabatic parameter close to one in fuel layer during implosion. Drive duration is constant in our study and size to correspond to the ablator thickness with laser power drive of 100 TW. Figure 1 (right) present laser pulses shapes initially defined for each aspect ratio target.

3 Optimization by random walk

Optimization consists to find the laser pulse shape that puts hot spot in optimal conditions to apply shock ignition scheme to have maximum gain. Three values are concerned in optimization, first one is the incident energy, second is the areal density when implosion velocity is under self ignition threshold, and third is the thermonuclear energy when implosion velocity is above self ignition threshold. Laser pulses shapes previously defined are not the most optimized pulse shape for a given implosion velocity.

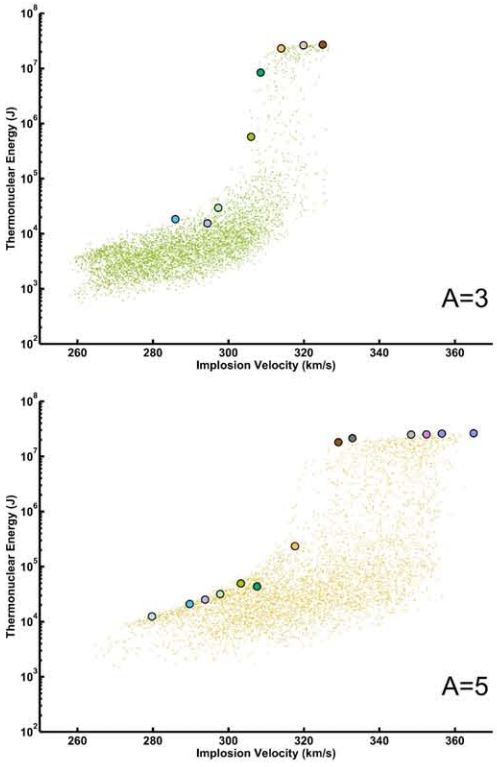

Fig. 2. Thermonuclear energy in function of implosion velocity for each aspect ratio A=3 (top) and A=5 (bottom). Colored points are selected working points optimized in areal density, thermonuclear energy and absorbed energy, that will be used to compute scaled targets.

We applied a random walk to find optimized laser pulse shape in function of implosion velocities. To do that, we defined intervals of time and power around each significant pulse shape point, and random power and time in these intervals to define a new laser pulse shape. This new laser pulse shape is integrated in computation code with target geometry. Successive refinements of intervals allow to explore underpopulated space. These refinements consist to find the trend of each points in the direction desired. We refined intervals to obtain lower implosion velocities with higher areal densities for A=5 computations, and to have more implosion velocities with maximum thermonuclear energies to exceed A=3 self ignition threshold. Global results in terms of thermonuclear versus implosion velocity

of many thousand of computations for each aspect ratio are reporting on Figure 2. We remark on this figure that self ignition threshold is around 310 km/s for A=3, and around 325 km/s for A=5. With the same fuel mass, self ignition threshold is reach with lower kinetic energy than A=5.

Implosion velocities range is large for each initial aspect ratio, but with the same absorbed energy, implosion velocities are globally lower for A=3 than A=5 target. In the two cases, self ignition threshold is reached, and maximum thermonuclear expected for 300 μg of DT fuel is obtained. Self ignition threshold is reached for lower implosion velocity for A=3. In fact, we explored the effect of kinetic energy variations only with implosion velocities. In next paragraph 4, we explored the mass variations of kinetic energy. Colored points on Figure 2 are the selected working points that we used to compute scaled targets.

4 Scaled targets

Working points have been selected in function of optimization criteria. These points offered the maximum areal density (under self ignition threshold) or maximum thermonuclear energy (above self ignition threshold), with minimum absorbed energy in function of implosion velocities. We report this points in the Table 1. As we remarked before, laser energy needed to reach an implosion velocity is higher for A=3 than A=5. But areal densities obtained are higher for A=3. Areal densities are around 1.88 g/cm^2 for A=3, and around 1.60 g/cm^2 for A=5.

A=3				A=5			
V (km/s)	E_a (kJ)	ρR (g/cm^2)	E_{th} (kJ)	V (km/s)	E_a (kJ)	ρR (g/cm^2)	E_{th} (kJ)
				280	171	1.46	12
286	215	1.85	18	**289**	181	1.50	21
294	233	1.88	15	**294**	187	1.53	25
297	238	1.84	29	**298**	193	1.56	32
306	234	1.86	573	**303**	199	1.58	49
308	250	1.87	8389	**308**	204	1.59	44
314	260	1.82	23032	**317**	219	1.59	234
320	272	1.86	26216				
325	283	1.89	26915	**329**	226	1.60	18 119
				333	233	1.64	21 411
				348	249	1.66	24 862
				352	264	1.64	25 064
				356	267	1.66	25 695
				365	280	1.67	26 296

Table 1. List of working points selected to compute scaled targets.

We search to find self ignition threshold for each working point. To do that, we will increase target mass, we apply a scaled transformation [18] that conserve velocities and laser intensities to explore kinetic energy in function of fuel mass at constant implosion velocity. In changing mass (i.e. varying scale factor) at constant implosion velocity, we change kinetic energy of the target and thermonuclear energy, new target move closer of self ignition threshold. Scaling law is expressed in follow with the scale factor f :

$$\frac{m_1}{m_0} = f,\ \frac{E_1}{E_0} = f,\ \frac{r_1}{r_0} = f^{1/3},\ \frac{t_1}{t_0} = f^{1/3},\ \frac{P_{laser\,1}}{P_{laser\,0}} = f^{2/3},$$
$$\text{and}\ \ \frac{V_1}{V_0} = 1,\ \frac{\rho_1}{\rho_0} = 1,\ \frac{I_1}{I_0} = 1$$

Scale factor is upper than one when working points are under self ignition threshold and lower than one if working points are above self ignition threshold. Results of these computations are reported on Figure 3 for each aspect ratio.

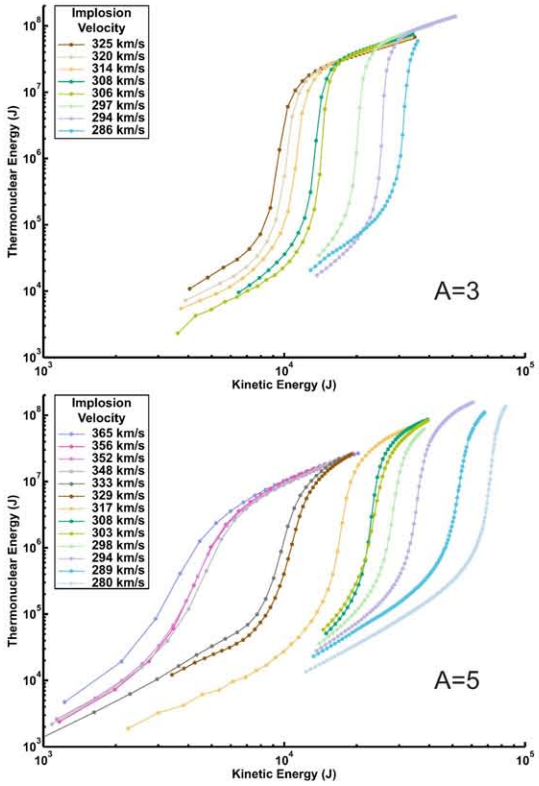

Fig. 3. Thermonuclear energy in function of kinetic energy for each aspect ratio A=3 (top) and A=5 (bottom), each point is a scaled target of a working point selected. Each line colored correspond to the scaled target of each working point. Implosion velocities are almost constant for each curve.

5 Shock ignition

Shock ignition scheme [10] consists to add a high power spike at the end of the drive pulse. This spike create a strong shock and cause ignition of assembled target that could not reach ignition without this spike. Self ignition threshold is reduce. Spike timing must be adjust precisely for the shock arrive at the most favorable moment to obtain high gain. More the kinetic energy of target is lower with regard of self ignition threshold, more the spike power will be higher.

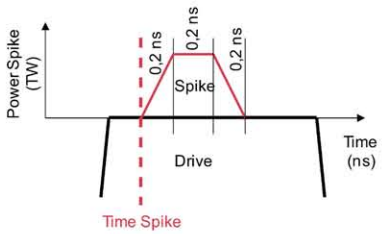

Fig. 4. Definition of spike added at the end of laser drive pulse in terms of timing and power.

We apply this method on a target that is under self ignition threshold on the A=5 target design with 317 km/s implosion velocity and have a kinetic energy around 10^4J, its scale factor is 0.7. Computations consisted to explore timing and power axes with a spike defined on the Figure 4. Results are presenting on a map of 1D gains function of power spike and time, on Figure 5. On the chosen target, we obtained a 1D gain of 93 with only 180 kJ of absorbed energy, thermonuclear energy free is close to 17 MJ.

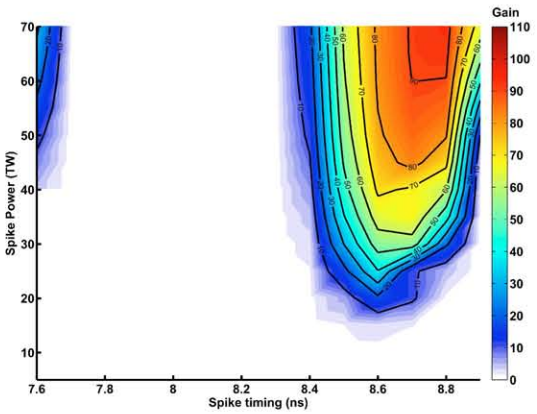

Fig. 5. Map of 1D gain obtained for a A=5, f=0.7, V=317 km/s, target design under self ignition threshold. Maximum gain is 93 for spike laser power of 65 TW at 8.8 ns. Thermonuclear energy is close to 17 MJ for 180 kJ of absorbed energy.

6 Conclusion

We defined two new targets design baseline with aspect ratio of 3 and 5, we explored large implosion velocities range with a random walk for each aspect ratio. Self ignition thresholds have been identified, and working points have been selected in function of thermonuclear energy, areal densities and absorbed energies. Comparison of working points of each aspect ratio reveals that absorbed energy is higher for lower aspect ratio at same implosion velocity but areal density is higher. We applied a scaling law that conserve implosion velocities on this working point that composed a large library of target design in function of aspect ratio, implosion velocity, fuel mass and position relative of self-ignition threshold. And finally, we apply shock ignition scheme on a target chosen in this library and obtain 1D gain around 93. Application of this scheme on all scaled targets will bring an added dimension at this library of target designs.

References

1. J. Nuckolls,L. Wood and A. Thiessen, Nature **269**, (1972) 139-142
2. J. D. Lindl, Physics of Plasmas **2**, (1995) 3933-4024
3. S. Atzeni and J. Meyer-ter-Vehn, *The Physics of Inertial Fusion. Beam Plasma Interaction, Hydrodynamics, Hot Dense Matter.* (Oxford University Press, Oxford, 2004) 450p.
4. J. D. Lindl, P. Amendt, R. L. Berger, S.G. Glendinning, S.H. Glenzer, S. W. Haan, L. Kauffman, L. Landen and L. J. Suter, Physics of Plasmas **11**, (2004) 339-491
5. S. E. Bodner, D. G. Colombant, A. J. Schmitt, J. H. Gardner, R. H. Lehmberg and S. P. Obenschain, Fusion Engineering and Design **60**, (2002) 93-98
6. B. Canaud, X. Fortin, F. Garaude, C. Meyer, F. Philippe, M. Temporal, S. Atzeni and A. Schiavi, Nuclear Fusion **44**,(2004) 1413
7. E. I. Moses, Energy Conversion and Management **49**, (2008) 1795-1802
8. J. Giorla, J. Bastian, C. Bayer, B. Canaud, M. Casanova, F. Chaland, C. Cherfils, C. Clique, E. Dattolo, P. Fremerye, D. Galmiche, F. Garaude, P. Gauthier, S. Laffite, N. Lecler, S. Liberatore, P. Loiseau, G. Malinie, L. Masse, A. Masson, M. C. Monteil, F. Poggi, R. Quach, F. Renaud, Y. Saillard, P. Seytor, M. Vandenboomgaerde, J. Van der Vliet and F. Wagon, Plasma Physics and Controlled Fusion **48**, (2006) 75-B82
9. B. Canaud, F. Garaude, C. Clique, N. Lecler, A. Masson, R. Quach and J. Van der Vliet, Nuclear Fusion **47**, (2007) 1652-1655
10. R. Betti, C. D. Zhou, K. S. Anderson, L. J. Perkins, W. Theobald and A. A. Solodov, Physical Review Letters **98**, (2007) 155001
11. B. Canaud and M. Temporal, New Journal of Physics **12**, (2010) 3037
12. S. Atzeni, A. Schiavi and C. Bellei, Physics of Plasmas **14**, (2007) 2702
13. E. Buresi, J. Coutant, R. Dautray, M. Decroisette, B. Duborgel, P. Guillaneux, J. Launspach, P. Nelson, C. Patou, J. M. Reisse and J. P. Watteau, Laser and Particle Beams **4**, (1986) 531
14. W. B. Hubbard, The Astrophysical Journal **146**, (1966) 858
15. V. Recoules, F. Lambert, A. Decoster, B. Canaud and J. Clerouin, Physical Review Letters **102**, (2009) 75002
16. L. Caillabet, B. Canaud, G. Salin, S. Mazevet and P. Loubeyre, Physical Review Letters **107**, (2011) 115004
17. R. E. Kidder, Nuclear Fusion **16**, (1976) 405-408
18. E. Falize, C. Michaut and S. Bouquet, The Astrophysical Journal **730**, (2011) 96